remote sensing

MDPI

Article

Monitoring and Analyzing the Effectiveness of the Effective Refuge Area of Emergency Shelters by Using Remote Sensing: A Case Study of Beijing's Fifth Ring Road

Di You [1,2], Shixin Wang [1,2], Futao Wang [1,2,3,*], Yi Zhou [1,2], Zhenqing Wang [1,2], Yanchao Wang [1,2], Jingming Wang [4], Yibing Xiong [5] and Jianwan Ji [6]

1 Aerospace Information Research Institute, Chinese Academy of Sciences, Beijing 100094, China; youdi@aircas.ac.cn (D.Y.); wangsx@aircas.ac.cn (S.W.); zhouyi@aircas.ac.cn (Y.Z.); wangzhenqing19@mails.ucas.ac.cn (Z.W.); wangyanchao191@mails.ucas.ac.cn (Y.W.)
2 University of Chinese Academy of Sciences, Beijing 100049, China
3 Hainan Research Institute, Aerospace Information Research Institute, Chinese Academy of Sciences, Sanya 572029, China
4 School of Geography and Ocean Science, Nanjing University, Nanjing 210023, China; wangjingming@smail.nju.edu.cn
5 School of Remote Sensing and Information Engineering, Wuhan University, Wuhan 430079, China; xiongyibing@whu.edu.cn
6 School of Geography Science and Geomatics Engineering, Suzhou University of Science and Technology, Suzhou 215009, China; jijw@usts.edu.cn
* Correspondence: wangft@aircas.ac.cn; Tel.: +86-134-264-025-82

Abstract: The effective refuge area is a key indicator in the study of emergency shelters. Accurately extracting the effective refuge area and analyzing the effectiveness of emergency shelters are of great significance for site selection, spatial distribution, and the evaluation of suitability. Beijing is one of only three capitals in the world located in a high-seismic-intensity zone of magnitude 8. The fast and accurate monitoring of effective refuge areas and an analysis of the effectiveness of emergency shelters are conducive to evacuation planning and disaster prevention and mitigation, and they promote the construction of a resilient city. However, the extraction of effective refuge areas in existing studies is not only a time-consuming and labor-intensive task but also has accuracy and efficiency problems, resulting in less precise validity analyses. In this paper, a remote sensing monitoring technology system for the effective refuge areas of emergency shelters is proposed based on multi-source data. Different methods were used to extract various land features, such as buildings and collapsed areas, water, dense areas of understory vegetation, and steep slope areas that cannot be evacuated, to obtain the effective refuge area at a detailed scale, in combination with the service radius of emergency shelters, the population distribution, and the actual road network, the criteria for effectiveness analysis were established for the effective open space ratio, capacity, per capita accessible effective refuge area, and population allocation gap. Taking the area within the Fifth Ring Road of Beijing as an example, the effectiveness of emergency shelters was analyzed at both the whole scale and a local scale. The results show that the effective refuge areas of different emergency shelters in Beijing vary significantly, with the smallest effective refuge area being located in Rings 2–3 and the largest one being located in Rings 4–5; between different regions, there are differences in the effectiveness. This study provides a feasible method for the fast, accurate, and detailed extraction of the effective refuge areas of emergency shelters and also provides a reference for emergency planning for disaster prevention and mitigation.

Keywords: remote sensing; emergency shelter; effective refuge area; effectiveness; deep learning; Beijing

check for updates

Citation: You, D.; Wang, S.; Wang, F.; Zhou, Y.; Wang, Z.; Wang, Y.; Wang, J.; Xiong, Y.; Ji, J. Monitoring and Analyzing the Effectiveness of the Effective Refuge Area of Emergency Shelters by Using Remote Sensing: A Case Study of Beijing's Fifth Ring Road. *Remote Sens.* **2023**, *15*, 3646. https://doi.org/10.3390/rs15143646

Academic Editor: Bruno Adriano

Received: 23 May 2023
Revised: 19 July 2023
Accepted: 19 July 2023
Published: 21 July 2023

1. Introduction

An emergency shelter is a place where open spaces, such as parks, green spaces, squares, sports fields, playgrounds, etc., are reasonably designed and renovated to meet the needs of emergency rescue facilities. These sites can provide shelters, rescue, and evacuation services for residents in the event of sudden disasters such as earthquakes [1,2]. Accurately extracting the effective refuge area of emergency shelters and analyzing their effectiveness are crucial for disaster prevention and emergency response preparedness. Such actions can help minimize the potential loss of lives and property damage, stabilize public sentiments, maintain the sustainable economic development of the city, and promote the construction of a resilient city [3,4].

According to the "Beijing Central City Earthquake and Emergency Shelters (Outdoor) Planning Outline" [5] and the "Beijing Local Standard: Design Specification for Emergency Shelter Function in Parks and Green Spaces (DB11/T794-2011)", the effective refuge area of emergency shelters is defined as the area that remains available for refuge use after excluding water areas, buildings, dense area of understory vegetation, areas of steep slopes greater than 7°, and areas affected by potential building collapse. Several methods can be used to obtain the effective refuge area of an emergency shelter: (1) estimating it to be 60% of the total site area. The "Beijing Central City Earthquake and Emergency Shelters (Outdoor) Planning Outline" recommends that the effective shelter area be calculated based on 60% of the floor area of the shelter [5]. Li et al. [6] estimated the effective refuge area of emergency shelters in the central urban areas of Beijing by calculating 60% of the site area and made recommendations for the construction of emergency shelters based on the population, supporting facilities, location, and road conditions. (2) Officially released statistical data. Wei et al. [7] obtained the effective refuge area of emergency shelters in Beijing on the basis of the actual investigation and statistical data of the Beijing Earthquake Bureau to evaluate the spatial distribution and service efficiency of emergency shelters from the perspectives of accessibility, fairness, and efficiency. Wang et al. [8] evaluated the spatial distribution of emergency shelters in Shanghai on the basis of officially released effective refuge area data. (3) Actual measurement. Tong [9] measured and verified the effective refuge area of park emergency shelters in Beijing, analyzed the current situation of park construction, and provided suggestions for improvement. Lv et al. [10] drew and calculated the effective refuge area of emergency shelters by using a measurement tool: the Water Conservancy Map Download Tool; they constructed a suitability evaluation index system from a public perspective and conducted a correlation analysis of the suitability and service range of emergency shelters. (4) Interpreting the situation with remote sensing images. Guo et al. [11] used remote sensing images to outline the scope of emergency shelters and areas where rescue cannot take place and those occupied by lakes and houses, obtained the effective refuge area, and analyzed the accessibility of park emergency shelters on the basis of the street population and buffer analysis. Zhou et al. [12] used SPOT satellite images, online maps, and textual information to visually interpret the effective refuge area of emergency shelters in Beijing and studied the rationality of emergency shelter spatial layouts at the community scale from the perspectives of accessibility and congestion. Zhang [13] computed the effective refuge area of emergency shelters in Urumqi by using remote sensing images, on-site investigations, and AutoCAD mapping. Zhong et al. [4] obtained the effective refuge area of emergency shelters through field investigations and remote sensing image interpretation; they optimized the spatial layout of urban emergency shelters based on spatial differences in the population, the age structure, and evacuation routes. (5) Automatic extraction. Xiao [14] used the buffer zone method to calculate the building collapse area, ArcGIS, to extract the steep slope areas with slopes greater than 7°, and AutoCAD for vectorization statistics for watershed and dense areas of understory vegetation to obtain the effective refuge area. Du et al. [15] extracted the refuge area in Yunnan using object-based classification methods based on GF-7 remote sensing images, unmanned aerial vehicle aerial imagery, and DSM digital elevation models.

The effective refuge area is a key indicator in research concerned with emergency shelter site selection planning, spatial layouts, and effectiveness analysis [16,17]. The effectiveness of emergency shelters refers to their ability to provide shelter for disaster victims during disasters [18]. The effectiveness of traditional emergency shelters is evaluated based on the effective refuge area inside the emergency shelter [8]. On this basis, other related indicators are extended to comprehensively analyze the effectiveness of emergency shelters. Xiao [14] used the effective shelter area and the per capita effective refuge area to represent the effectiveness of shelters and selected seven demonstration areas for a comparative analysis of effectiveness. Xiong [19] constructed an evaluation index system from the internal functional zoning, road traffic, and disaster prevention facilities of the shelter site to evaluate the effectiveness of park emergency shelters. Wang et al. [8] reflected the emergency shelter supply capacity of Shanghai under the current spatial distribution of emergency shelters through three indicators: the service scope, the number of people served, and the service overlap area ratio. Yao [20] combined the emergency shelter spatial distribution, area, and population mobility to reflect the availability of emergency shelters in Victoria. Yu et al. [21] selected the factors of area, capacity, and service area to reflect the spatial distribution and effectiveness of emergency shelters for evacuation in Shanghai. Alawi et al. [22] reflected the effectiveness of emergency shelters through the per capita effective shelter area. Chen et al. [23] analyzed the effectiveness of emergency shelters using the ratio of the number of accommodated refugees to the opening space.

The above studies have made beneficial attempts to calculate the effective refuge area and analyze the effectiveness of emergency shelters. However, the following problems still need to be further addressed and improved: (1) There are different levels of specificity for the definition of the effective refuge area; for instance, the effective refuge area calculation process does not exclude buildings, water, or dense areas of understory vegetation and other areas that cannot provide refuge, and the insufficient accuracy in various methods of feature extraction leads to significant errors in the results related to effective refuge areas. (2) The accuracy and efficiency of calculating the effective refuge area of emergency shelters need to be improved. With the improvement of remote sensing image resolution and the rapid development of artificial intelligence technology, the use of remote sensing technology can quickly, accurately, and intelligently extract relevant element information, which could improve the monitoring efficiency of the effective shelter area [24,25]. (3) The effective refuge area of emergency shelters is not considered comprehensively and precisely enough, which means that the effectiveness analysis of emergency shelters could be improved in terms of scientificity and objectivity.

In summary, to address the above problems, this paper uses multiple sources of data, such as remote sensing images, aerial images, and Baidu electronic maps, according to the definition of the effective refuge area of emergency shelters; it also uses various extraction methods, such as deep learning, machine learning, and field research, for different features to construct a remote sensing monitoring technology method system to determine the effective refuge area of emergency evacuations. This system can extract the effective shelter area accurately, quickly, and in detail. At the same time, based on the effective refuge area, we combine the service radius, road accessibility, and population distribution of emergency shelters and construct four indicators—the open space ratio, capacity, per capita accessible effective refuge area, and population allocation gap—to comprehensively analyze the effectiveness of emergency shelters from both a regional perspective and an overall perspective, taking Beijing's Fifth Ring Road as an example.

This paper is organized as follows. Section 2 introduces the study area and the datasets used. Section 3 proposes a remote sensing monitoring technique system for the effective refuge area of emergency shelters and designs criteria for an effectiveness analysis, including the EfficientUNet+ deep learning model, the object-oriented classification method, field investigation, and four indicators for effectiveness analysis. Section 4 conducts experiments with the proposed method, obtaining the area of buildings and areas characterized by collapsed water-dense areas of understory vegetation, and steep slopes in order to determine

the effective refuge area and conduct contrastive verification. Section 5 analyzes the effectiveness of emergency shelters from the perspectives of the open space ratio, capacity, per capita accessible effective refuge area, and population allocation gap. Section 6 summarizes the article's findings and shortcomings and proposes future research prospects.

2. Study Area and Data

2.1. Study Area

Beijing, the capital city of China, covers an area of 16.4 km^2 and is the political and cultural center of China with an important geographical position in both China and the world. It is adjacent to the Yan Mountains in the north, borders the Taihang Mountains in the west, and is in the Yinshan–Yanshan seismic belt, which is the main earthquake zone in north China. According to historical records, Beijing has experienced nearly 200 earthquakes with a magnitude greater than 4, more than 10 earthquakes with a magnitude greater than 5, and even a massive magnitude 8 earthquake, making this area a key defense city for disaster prevention and mitigation in China. The central urban area of Beijing has a high concentration of buildings and a high-population density, where old and new buildings coexist. The destructive power of a disaster would be much greater here than in other areas. This situation may lead to the collapse of a large number of buildings and to numerous casualties, and even secondary disasters after the earthquake, such as fires, floods, and the spread of hazardous substances and toxins, thereby paralyzing the entire urban system. This paper focuses on the emergency shelters within Beijing's Fifth Ring Road. According to the list of emergency shelters published by the Beijing Emergency Management Bureau in 2022, 59 emergency shelters are found within the Fifth Ring Road, including 44 park-type shelters, 6 green-space-type shelters, and 9 sport stadium-type shelters. The spatial distribution of emergency shelters in the study area is shown in Figure 1.

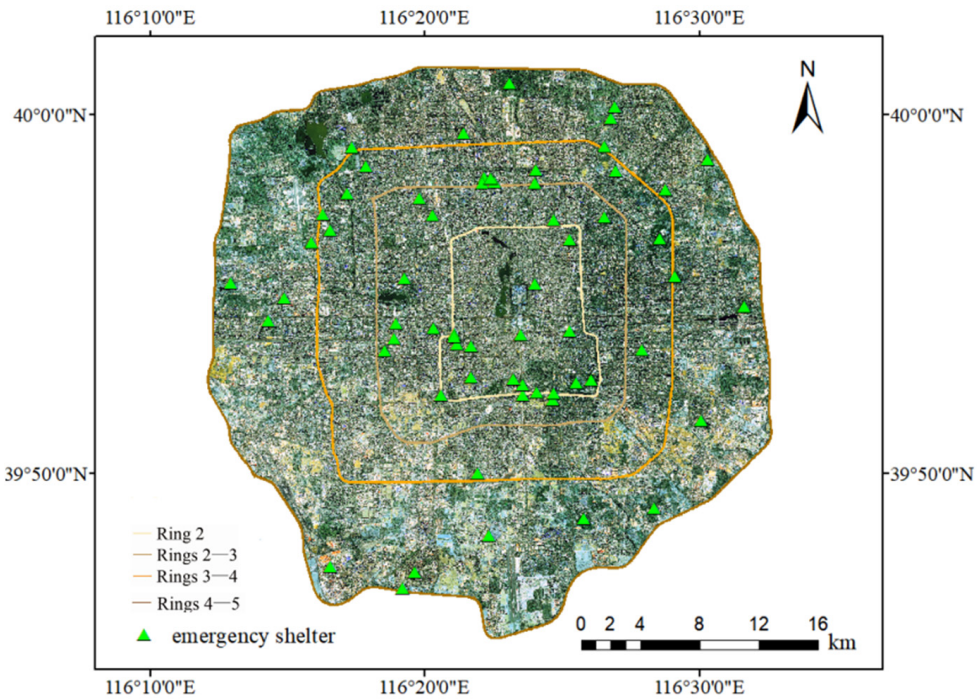

Figure 1. Spatial distribution of emergency shelters within Beijing's Fifth Ring Road.

2.2. Data and Pre-Processing

On the basis of the list of emergency shelters published by the Beijing Emergency Management Bureau in 2022, this study uses data that include the administrative divisions of Beijing, Baidu electronic maps, GF-2 remote sensing images, DEM images, Google Images, WHU building datasets, population data, and road networks, as shown in Table 1.

The location range of emergency shelters was obtained using Baidu's web crawlers and was registered and interpreted to establish a vector database of emergency shelter boundaries for this study. The GF-2 remote sensing images used in this study were pre-processed by radiation calibration, atmospheric correction, fusion, stitching, and cropping, resulting in high-resolution remote sensing images with a spatial resolution of up to 1 m, which cover the area within the Fifth Ring Road of Beijing. After undergoing pre-processing, the image data retain good levels of color, texture, and spectrum, with less cloud cover and high-quality imaging, which is conducive to information extraction [26]. The GF-2 green space dataset from researcher Xu Zhiyu [27,28] was used and divided into grassland and other green space for the extraction of dense areas of understory vegetation, according to the research needs.

Table 1. List of data required for this paper.

No.	Name	Source	Resolution	Format
1	List of emergency shelters	Beijing Emergency Management Bureau official website (http://yjglj.beijing.gov.cn, accessed on 30 March 2022)	—	Text
2	Beijing administrative district	National Basic Geographic Information Center	—	Vector
3	Baidu electronic map	https://map.baidu.com, accessed on 8 May 2022	—	Raster
4	GF-2 remote sensing image	China Centre for Resources Satellite Data and Application (https://data.cresda.cn, accessed on 8 May 2022)	1 m	Raster
5	DEM images	ALOS PALSAR Products	12.5 m	Raster
6	Google images	Google Map	0.23 m	Raster
7	GF-2 green space dataset	Xu et al. [27,28]	1 m	Raster
8	WHU building dataset	http://study.rsgis.whu.edu.cn/pages/download/, accessed on 8 May 2022	0.3 m	Raster
9	Street population	Seventh National Population Census Bulletin	—	Text
10	Beijing road network	Electronic Map Data in 2022	—	Vector

3. Methods

In China, emergency shelters are typically outdoor open spaces converted from parks, playgrounds, squares, sport fields, and green spaces. At their inception, the shelters were not originally designed for emergency purposes, and their internal facilities have gradually been updated over time, resulting in changes to the effective shelter area. As emergency shelters are places for post-disaster concentrated rescue and evacuation, their effective shelter area needs to be monitored quickly and dynamically to more accurately analyze the effectiveness of emergency shelters and to help improve post-disaster planning. To meet these needs, this paper proposes a remote sensing monitoring technology system for assessing the effective refuge area of emergency shelters at a fine scale on the basis of multi-source data. Various methods were adopted for the accurate and efficient extraction of information to account for buildings and collapsed areas, bodies of water, dense areas of understory vegetation, and steep slopes that cannot be used as refuges. Moreover, on the basis of the effective refuge area, combined with the service scope, population distribution, and practical road networks, this study established criteria for analyzing the effectiveness of emergency shelters and conducted a more accurate, scientific, and comprehensive analysis to enable the relevant departments of China to improve disaster prevention and evacuation capabilities and urban security. The technical process is shown in Figure 2.

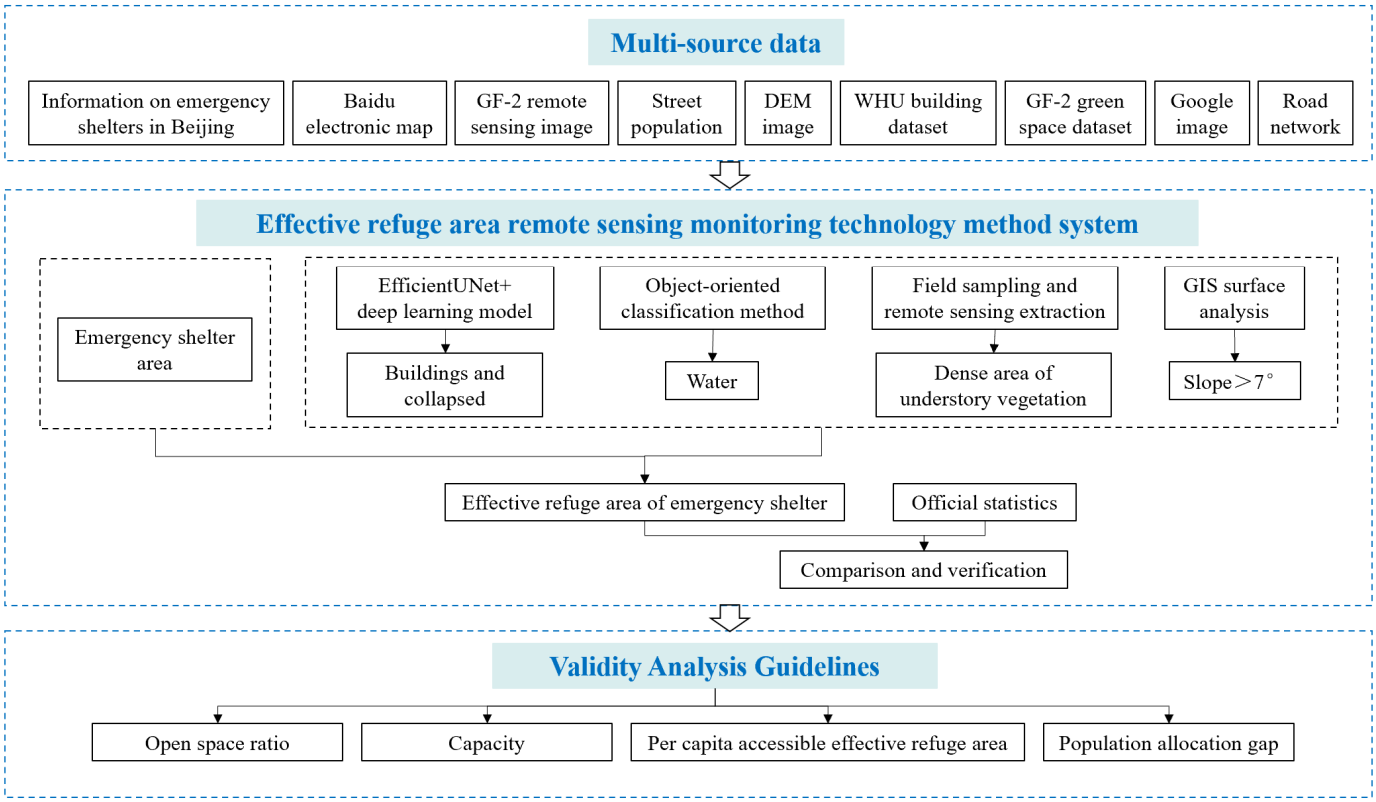

Figure 2. Technology roadmap.

3.1. System Based on the Remote Sensing Monitoring Technology Method for the Effective Refuge Area

3.1.1. Building an Extraction Model from EfficientUNet+ Deep Learning

Building emergency shelters is characterized by small footprints and their small volume, which can easily cause issues such as misdetection, false detection, and boundary blurring to occur when using remote sensing imagery for building extraction. EfficientUNet+ [29] is a deep learning model of fully convolutional neural networks. On the basis of the overall framework of the encoder–decoder of the UNet model and with the use of a skip-connection method, it can better integrate the high-level and low-level semantic information of the network, restore fine edges, and quickly, accurately, and fully extract buildings (Figure 3). Multi-scale features can be obtained by subjecting the convolutional neural network structure to deepening, widening, and increasing the model input size. As the network layers become deeper and wider, problems such as gradient fading and overfitting may occur. However, EfficientUNet+ uses EfficientNet as the model encoder, which uses composite coefficients to uniformly scale the three dimensions of width, depth, and resolution, with fewer parameters, faster operation speeds, and better robustness, and it can effectively learn the deep semantic information of images [30]. At the same time, the decoder of EfficientUNet+ is embedded with a spatial channel attention mechanism (scSE), which can emphasize significant positional information and improve extraction accuracy [31]. The problem of blurred boundary extraction can be solved because EfficientUNet+ also uses a cross-entropy function to weight the boundary areas and combines dice loss to strengthen the constraint of the boundary.

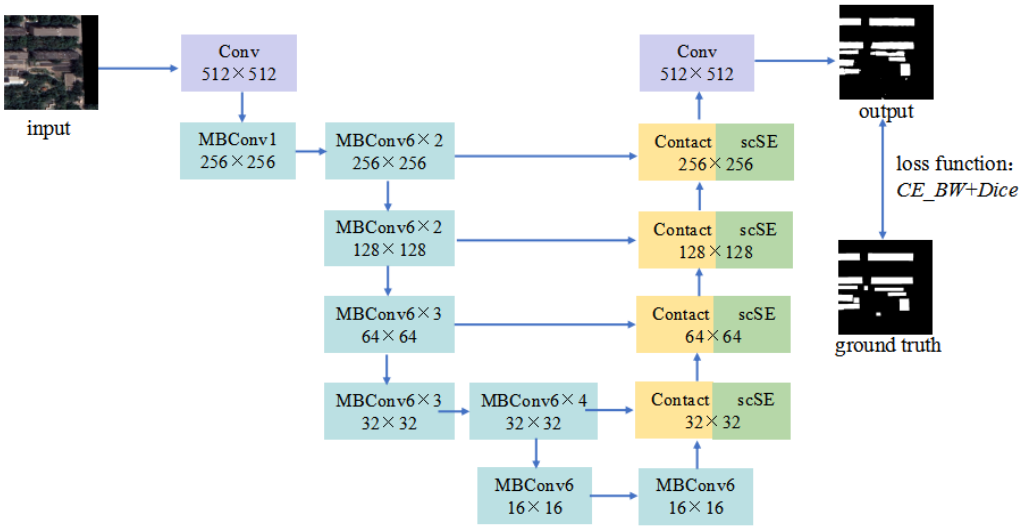

Figure 3. The EfficientUNet+ model (Adapted with permission from Ref. [29]. 2022, You, D. et al.).

3.1.2. Water Extraction Method of Object-Oriented Classification

Twenty-four emergency shelters with water are present within the area enclosed by the Fifth Ring Road in Beijing, all of which are distributed in parks. Considering that the water area in the park is smaller than natural lakes and that the number of training samples is limited, and that the water in the park mainly comprises lakes that form relatively large block-shaped bodies, which are easier to extract than buildings, this paper adopts an object-oriented classification method to extract water inside emergency shelters. The object-oriented classification method takes regionally homogeneous objects as the classification units and considers texture, spectral and spatial multidimensional features. This method is not only simple and efficient but also overcomes the "salt-and-pepper" phenomenon that occurs when extracting information using pixel-based classification methods. This method has obvious advantages in high-resolution remote sensing image classification [32,33] and can effectively extract water in emergency shelters.

NDWI is a commonly used water index that is sensitive to water and can effectively extract it. Considering that the water in the park mainly comprises large block-like bodies, setting an area threshold can eliminate interference from small water bodies. Moreover, water exhibits strong absorption characteristics in the near-infrared band, and the difference in the grayscale value between water and other land objects is largest in the near-infrared band. Thus, water can be effectively separated from non-water objects.

On the basis of the above conditions, an object-oriented machine learning method based on rules is established to extract water from emergency shelters according to experience values: (1) NDWI > 0.1; (2) area > 40 m^2; (3) b4 < 250. Small objects such as bridges, islands, and boats often obstruct the water in parks. Thus, morphology operations are performed on the extracted water, first by dilation and then by erosion, to identify water that cannot be used for refuge (Figure 4).

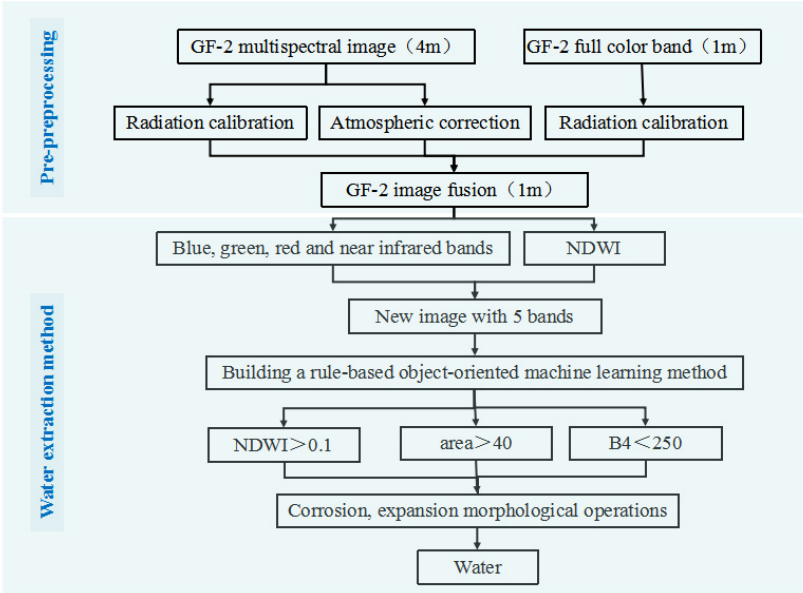

Figure 4. Object-oriented water extraction technology approach.

3.1.3. Experimental Design and Calculation Method for Dense Areas of Understory Vegetation

Dense areas of understory vegetation mainly comprise plant species below 4 m, such as shrubs, small trees, ground-cover plants, and grasses [34]. In landscape planning, such areas are often used to form a diverse and staggered plant community. Considering that the dense area of understory vegetation is mostly covered by tall trees, extracting it using remote sensing images alone is difficult. Therefore, this paper adopts field investigations to design an experimental plan and combines remote sensing image data to calculate the proportion of the dense area of understory vegetation that cannot be used for refuge in emergency shelters. Thus, the area occupied by the dense area of understory vegetation can be estimated. The experimental plan is as follows:

(1) The emergency shelter is divided into the forest type and the common type, and representative shelters for field inspection are selected. Forest type: Olympic Forest Park. Common type: Chaoyang Park, Haidian Park, and Jiangfu Park.

(2) Plot survey: The plot area is 20 m × 20 m, which expands 10 m from the central point in all directions.

(3) Measurement methods: The tools used include rulers, pedometers, image maps, recording sheets, and GPS.

On the basis of the distribution of green spaces in remote sensing images, low-, medium-, and high-vegetation cover areas were selected, and sampling points were selected in advance to ensure the uniform distribution of the sampling points. Then, the field location was determined based on the image; a sample was taken by expanding 10 m in all directions from the central point, and the area occupied by the dense area of understory vegetation within the 400 m^2 plot was measured. Then, the area of green space in the sample area other than the lawn was extracted from the GF-2 remote sensing image [27,28], the ratio of the area occupied by the dense area of understory vegetation to other green space was calculated for each sample, and the average was calculated.

$$S_g = \sum_{i=1}^{N} (S_m / S_r) / N \tag{1}$$

where S_g represents the area occupied by the dense area of understory vegetation, S_m represents the area occupied by the dense area of understory vegetation in the measured

plot, S_r represents the area of other green spaces in the corresponding sample on the remote sensing image, and N represents the number of samples.

3.2. Design of Guidelines for Emergency Shelter Effectiveness Analysis

The effectiveness of emergency shelters reflects the efficiency and supply capacity of refuge points during disasters. Emergency shelters should not only provide residents with accommodation, supplies, and rescue services but also meet people's needs for refuge spaces [35]. Generally, the effectiveness of shelters is reflected by the effective refuge area [8], but assessing effectiveness based solely on this indicator can produce a relatively one-sided analysis. This paper considers the service radius of the refuge, road accessibility, and the population distribution, and establishes effective analysis criteria, namely four indicators: the open space ratio, capacity, the per capita accessible effective refuge area, and the population allocation gap. A comprehensive analysis of the effectiveness of emergency shelters is conducted based on these criteria.

3.2.1. Open Space Ratio

The open space ratio refers to the ratio of the effective refuge area to the area occupied by the shelter. A large proportion corresponds to the shelter having a large usable area and improved openness [36].

$$a = S_e / S_E * 100\% \tag{2}$$

where a represents the open space ratio, S_e represents the effective refuge area, and S_E represents the area occupied by the refuge.

3.2.2. Capacity

Capacity refers to the ratio of the effective refuge area to the per capita effective refuge area in the refuge. The more people it can accommodate, the higher the supply capacity of the shelter [37]:

$$V = S_e / S_{ave} \tag{3}$$

where V represents the capacity, S_e represents the effective refuge area, and S_{ave} represents the per capita effective refuge area.

3.2.3. Per Capita Accessible Effective Refuge Area

The per capita accessible effective refuge area refers to the effective refuge area that is accessible to each person in the study area, reflecting the fairness of the spatial distribution of shelters [38]:

$$F = S_e / S_T \tag{4}$$

where F represents the per capita accessible effective refuge area, S_e represents the effective refuge area, and S_T represents the total population within the service area.

The service range of a shelter refers to the distribution range of shelter personnel that can be provided with emergency refuge [39]. When analyzing the service range of a shelter, traditional buffer zone methods use the spatial straight-line distance as the radius of the buffer without considering the effect of roads on travel [2]. Network analysis can calculate the distance between two points based on actual road data. It can objectively evaluate the accessibility and convenience of the shelter to residents by reflecting the actual travel routes from the demand point to the shelter [8,40,41]. This paper uses the network analysis module of the ArcGIS platform to calculate the service range of emergency shelters on the basis of the actual road length between the supply point of the emergency shelter and the demand point of the residents who need refuge.

3.2.4. Population Allocation Gap

The population allocation gap refers to the difference between the total population in the study area that needs refuge and the total population that can be accommodated in

existing shelters within a certain service radius. It reflects the matching degree of shelter facilities [7].

$$S_G = S_D - \sum S_P(d_{ij} \leq r) \tag{5}$$

where S_G represents the population allocation gap, S_D represents the total population in the study area that needs refuge, $\sum S_P$ represents the total population that can be accommodated in the existing shelters, and r represents the service radius. When S_G is 0 or less than 0, then no population allocation gap exists, and existing shelters can accommodate residents who need refuge.

4. Results

4.1. Effective Refuge Area Extraction Results

4.1.1. Building and Collapsed Area Extraction Results

When using the EfficientUNet+ deep learning method to extract emergency shelter buildings, obtaining sufficient building samples can ensure that the deep learning model is fully trained and that it can be used to efficiently extract buildings within emergency shelters in subsequent research. Visual interpretation based on satellite images is a commonly used method for sample collection. However, the number of building samples obtained for the study area is still insufficient. In consideration of the publicly available WHU building sample dataset, transfer learning can be used to apply it to model training. Therefore, this study uses the WHU building dataset and a self-made building sample dataset of the study area for visual interpretation using Google images (Figure 5).

Figure 5. Building samples from the WHU dataset and Google images. (**a**) Building sample from the WHU dataset. (**b**) Building samples from Google images.

Considering the limited number of building samples for emergency shelters, this paper uses the transfer learning method and EfficientUNet+ to train the publicly available WHU building dataset and then extract the buildings within the emergency shelters within the Fifth Ring Road of Beijing. Taking the Olympic Forest Park emergency shelter as an example, the building extraction results are shown in Figure 6. As shown in Figure 6, all the buildings inside the emergency shelter are extracted with clear boundaries, except for a few buildings that are not recognized because of occlusion by other objects.

According to the "Urban Comprehensive Disaster Prevention Planning Standards" (GB/T 51327-2018), the maximum range of the impact of building collapse is between one-half and two-thirds of the building height [42,43]. According to the "National Residential Design Standards" and the "Urban Primary and Secondary School Building Standards", the collapsed area of buildings in park-type or green-space-type emergency shelters is buffered by 1.5 m from the building's boundaries, while the collapsed area of buildings in square-type emergency shelters is buffered by 6 m from the building boundaries. The collapse areas are fused to prevent them from overlapping, which may cause an overestimation of the area. Taking the emergency shelter of the Affiliated Primary School of Beijing Normal University as an example, the building collapse extraction results are shown in Figure 7.

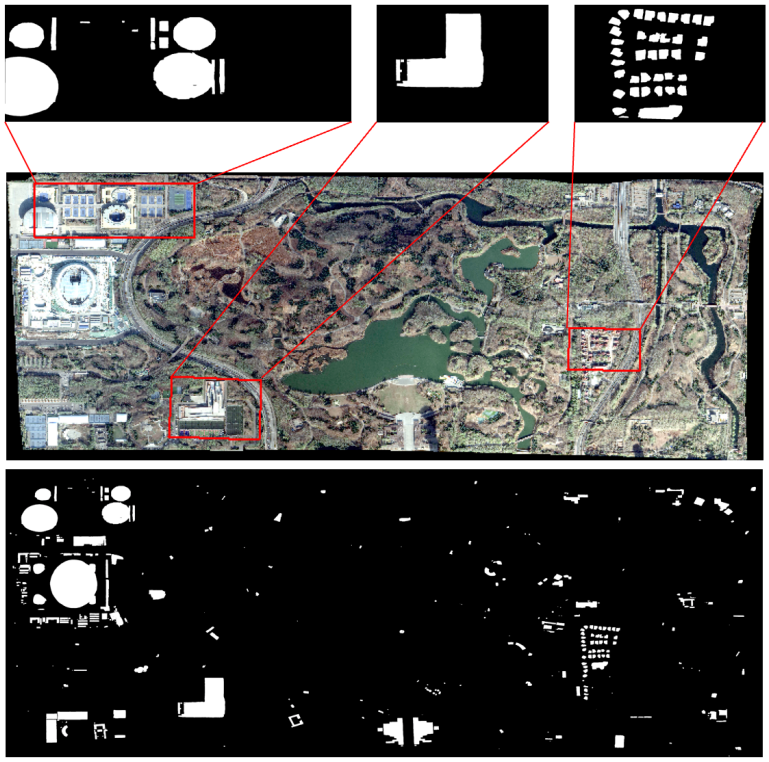

Figure 6. Results of building extraction for the Olympic Forest Park emergency shelter.

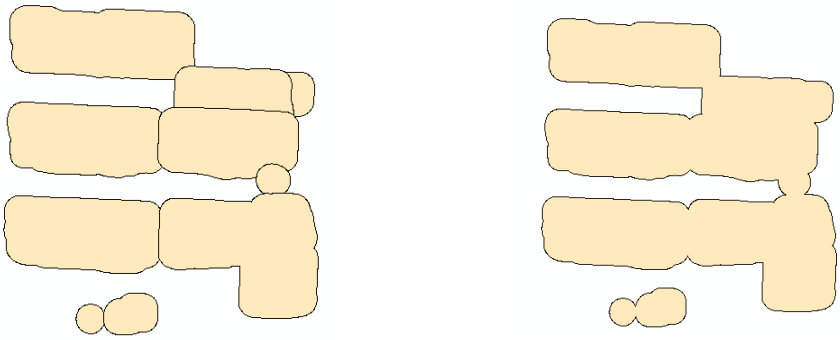

(**a**) (**b**)

Figure 7. Extraction results of some buildings and the collapsed area of the emergency shelter of the Affiliated Primary School of Beijing Normal University. (**a**) Extraction results of buildings and collapsed areas. (**b**) Extraction results of buildings and collapsed areas after fusion.

4.1.2. Water Extraction Results

A rule-based object-oriented classification method is established based on the ENVI platform and using GF-2 high-resolution remote sensing imagery. According to empirical values, NDWI > 0.1, area > 40 m^2, and b4 < 250 are used as constraints, and then morphological operations are used to remove small objects such as bridges, islands, and ships. With the Olympic Forest Park emergency shelter taken as an example, the water extraction results within the emergency shelter are shown in Figure 8.

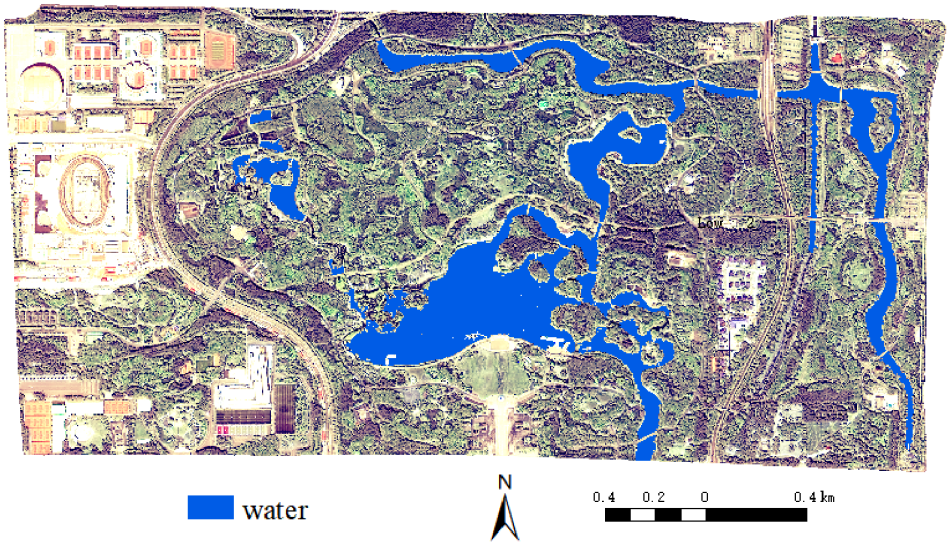

Figure 8. Results of water extraction for the Olympic Forest Park emergency shelter.

4.1.3. Dense Areas of Understory Vegetation Extraction Results

According to the field investigation plan designed in this paper, the representative emergency shelters—Olympic Forest Park (forest type) and Chaoyang Park, Haidian Park, and Jiangfu Park (non-forest type)—were selected as sample areas for field investigation. Olympic Forest Park is the largest forest park within the Fifth Ring Road of Beijing; thus, it was selected as being representative of forest-type emergency shelters. Similarly, because Chaoyang Park and Haidian Park are large-scale, non-forest-type emergency shelters within the Fifth Ring Road of Beijing, and Jiangfu Park is an emergency shelter newly included by the Beijing Municipal Emergency Management Bureau in 2022; they are selected as the representative non-forest-type emergency shelters in this paper. The distribution of the sampling points is shown in Figure 9.

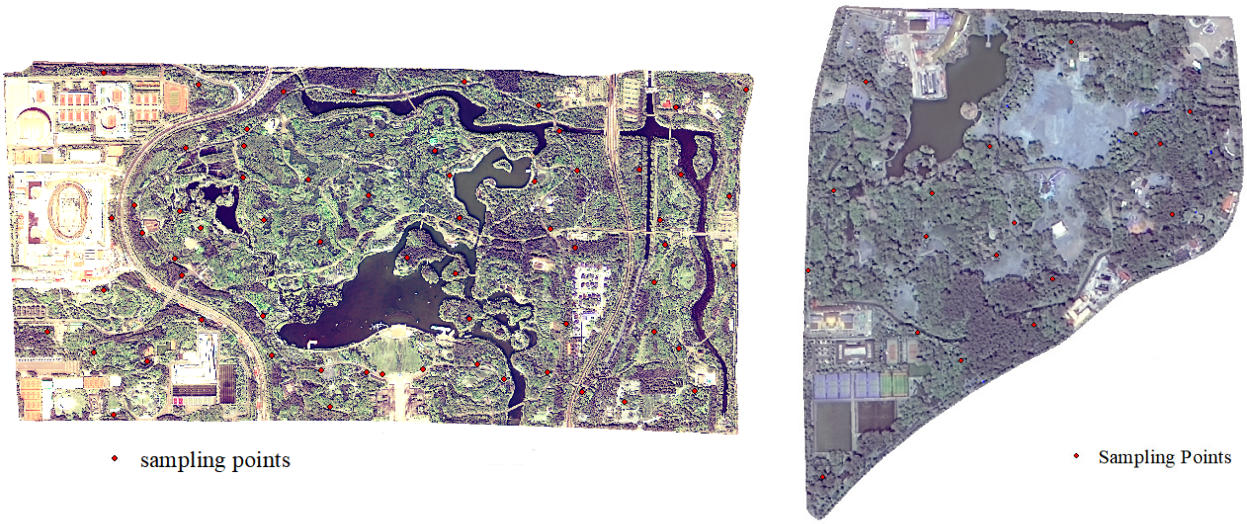

(**a**) (**b**)

Figure 9. *Cont.*

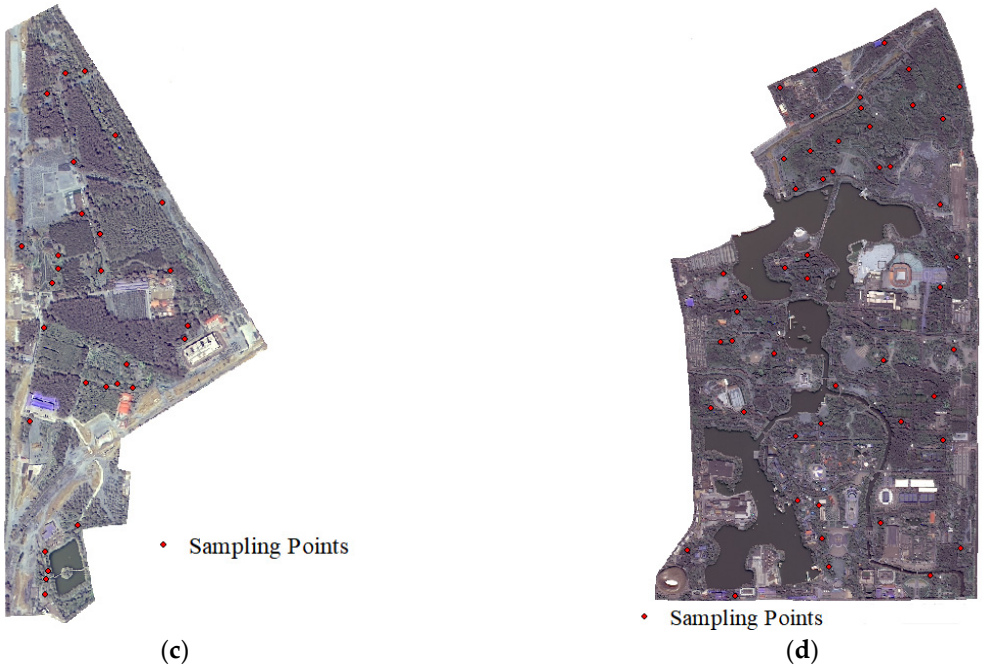

Figure 9. Field trip sampling sites in the dense area of understory vegetation of emergency shelters. (**a**) Sampling sites of Olympic Forest Park. (**b**) Sampling sites of Chaoyang Park. (**c**) Sampling sites of Haidian Park. (**d**) Sampling sites of Jiangfu Park.

A total of 160 sampling points are uniformly distributed in each emergency shelter, and the area occupied by the dense area of understory vegetation in each sampling plot was measured through field investigations. On the basis of the coordinates of the sampling points and the green-space extraction results from the GF-2 remote sensing images published by Xu et al. [27,28], the area of green spaces other than grassland within each sampling plot was extracted from the corresponding positions in the image. With the Olympic Forest Park emergency shelter taken as an example, the results of extracting the dense areas of understory vegetation are shown in Figure 10, while the results of a single sampling plot are shown in Figure 11. According to Formula (1), the area of the dense areas of understory vegetation, compared with other green spaces in each sampling plot, was determined to have an average proportion of 29.66%. The calculated areas of the dense area of understory vegetation in each emergency shelter are shown in Table 2 (see Section 4.1.5).

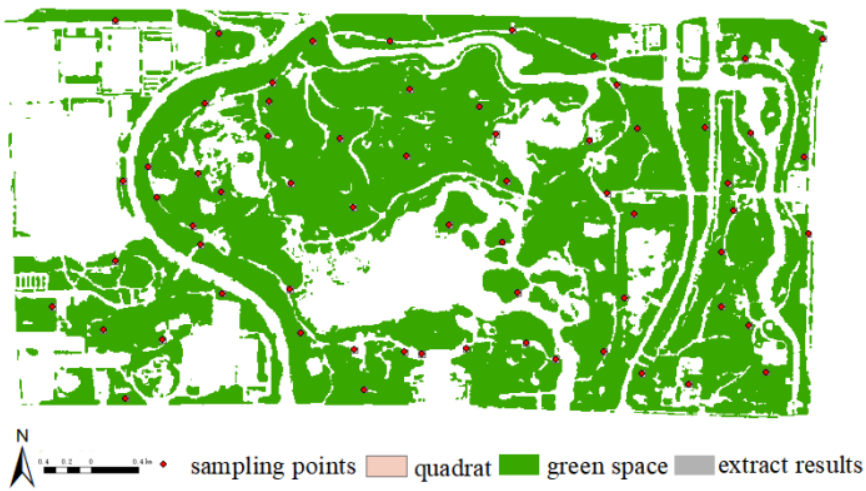

Figure 10. Extraction results of the dense areas of understory vegetation for the Olympic Forest Park emergency shelter.

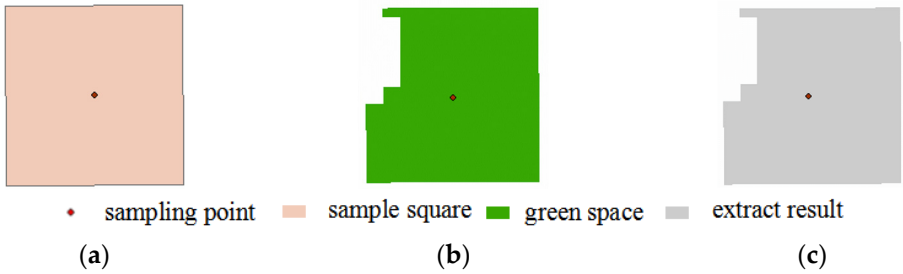

Figure 11. Sample square and corresponding green space image and extraction results. (**a**) Sample square. (**b**) Green space image dataset. (**c**) Extraction result.

4.1.4. Slope Extraction Results

The surface analysis tool on the ArcGIS platform was used to calculate the slope based on the DEM imagery. Then, the slope was reclassified to extract areas with slopes greater than 7°. The result is shown in Figure 12.

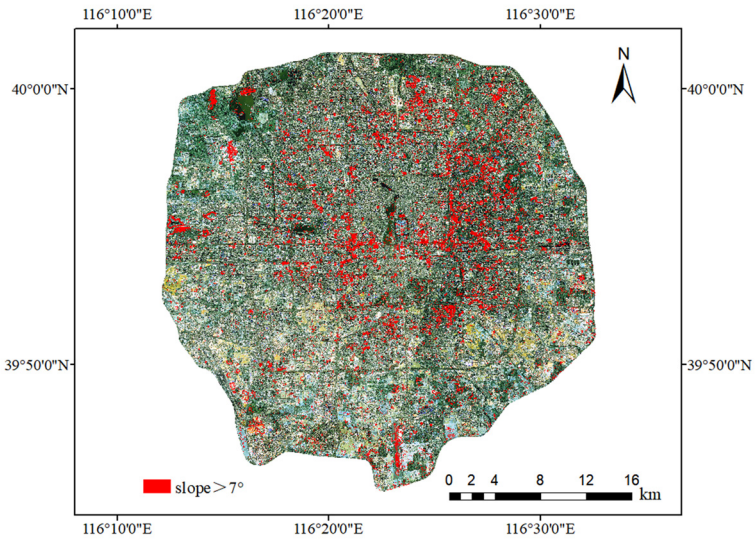

Figure 12. Extraction results of the slopes > 7° of emergency shelters within the Fifth Ring Road of Beijing.

4.1.5. Effective Refuge Area

The effective refuge area is calculated by the following formula:

$$S_e = S_E - S_b - S_w - S_g - S_s \tag{6}$$

where S_e represents the effective shelter area, S_E represents the area occupied by emergency shelters, S_b represents the area of buildings and their collapsed areas, S_w represents the area of water, S_g represents the area occupied by the dense area of understory vegetation, and S_s represents the area where the slope is greater than 7°.

The area occupied by each emergency shelter was calculated based on the vector boundaries of the emergency shelter range. Simultaneously, in reference to the areas of buildings and their collapsed areas, water bodies, dense areas of understory vegetation, and areas where the slope is greater than 7° that were extracted from emergency shelters within the Fifth Ring Road in Beijing, the effective shelter area within this area was calculated according to Formula (6). The effective shelter areas within different rings were calculated and summarized as shown in Table 2.

Table 2. Statistical table of the effective refuge areas of emergency shelters.

Location	Name	Type	Building and Collapsed Areas (m^2)	Water (m^2)	Slope > 7° (m^2)	Dense Area of Understory Vegetation (m^2)	Effective Refuge Area (m^2)	Percentage (%)
Ring 2	Huangchenggen Heritage Park	III	523.70	0.00	1406.25	18,901.77	57,956.92	73.56
	Ming City Wall Heritage Park	II	6206.51	0.00	14,218.75	20,661.92	76,989.81	69.23
	Yuting Park	II	10,185.13	18,526.11	1406.25	5078.38	35,853.84	65.20
	South Central Green Space	II	9659.96	0.00	2968.75	0.00	122,151.75	50.46
	South Central Road Green Space North Land	III	739.46	0.00	7031.25	0.00	20,330.42	90.63
	Nanguan Park	II	1060.03	2510.43	1406.25	3902.07	18,282.69	72.35
	Longtan Park	III	24,845.64	146,038.28	70,625.00	47,633.36	101,332.28	67.31
	Longtan West Lake Park	III	65,244.85	41,055.76	50,468.75	91,454.66	330,981.93	25.95
	Qianmen Arrowhead Green Space	III	4416.98	0.00	19,062.50	0.00	208.93	57.14
	Twenty-four Solar Terms Park	II	489.50	0.00	2812.50	1595.04	21,555.85	52.58
	Shennongtan Shencang Outer Green Space	III	215.26	0.00	0.00	1282.41	3570.98	0.88
	Cuifangyuan Green Spac	III	1886.66	0.00	4218.75	1442.75	1384.52	81.49
	Jinzhongdu Park	I	4788.29	0.00	6875.00	9431.06	35,801.43	70.45
	Wanshou Park	III	3377.56	274.56	781.25	8783.75	29,439.25	15.50
	Xibianmen Green Space	III	655.33	0.00	7656.25	5773.38	17,359.20	65.24
	Changchunyuan Park	III	4313.80	0.00	8125.00	1153.66	3264.33	62.92
	Xuanwu Yiyuan Park	II	3173.05	1694.10	156.25	14,976.45	44,954.79	69.01
	Beijing Experimental School (Haidian)	II	17,871.02	0.00	0.00	0.00	17,627.80	55.21
Rings 2–3	Ditangyuan Waiyuan	III	1348.24	0.00	5468.75	12,023.60	42,383.75	19.37
	Xiangheyuan Green Space	III	4748.70	0.00	11,406.25	16,383.74	36,085.63	69.21
	Baiyun Park	III	1170.83	0.00	0.00	1991.71	8053.39	71.80
	Beijing West Station Sunken Plaza	II	2462.34	0.00	0.00	0.00	8617.16	50.41
	Jiaotong University Affiliated High School	II	19,576.39	0.00	24,843.75	0.00	14,112.92	41.98
	Beijing Yu Yuan Tan Middle School	III	9500.54	0.00	0.00	0.00	3101.21	68.06
	Yixin Gargen	III	562.37	0.00	312.50	1845.98	8329.71	64.32
	Lotus Pond Park	I	5884.49	113,615.82	60,468.75	45,125.76	176,524.76	61.63
Rings 3–4	Rose Park	III	2273.81	0.00	2968.75	7099.60	23,165.11	40.26
	Yuan Dadu City Wall Ruins Park	I	73,779.32	52,775.55	54,843.75	99,715.08	285,793.12	66.06
	Chaoyang Park	I	172,357.56	434,187.87	628,281.25	426,022.80	1,201,785.95	76.60
	Sun Palace Park	I	12,194.54	21,500.02	85,625.00	40,042.91	339,640.81	71.61
	Xidawang Road Community Park	II	95.99	0.00	0.00	3232.10	15,415.44	67.55
	Anzhen Yongxi Park	III	2451.84	0.00	4843.75	793.94	2451.22	82.24
	Shuguang Disaster Prevention Education Park	II	1190.99	1213.49	937.50	11,836.44	35,137.62	23.25
	Madian Park	III	900.81	0.00	12,500.00	16,879.65	44,649.79	83.08
	Changchun Fitness Park	III	177.92	0.00	156.25	17,135.66	58,067.15	75.02
	Haidian District National Primary School	III	10,802.42	0.00	5312.50	0.00	3517.17	72.69
	Beijing Haidian District Teachers' Training School	III	19,442.00	0.00	625.00	0.00	1401.11	69.83
	Linfeng Park	III	847.69	0.00	0.00	1922.57	5552.38	77.78
Rings 4–5	Olympic Forest Park	II	230,549.37	353,174.39	104,218.75	663,874.61	2,437,241.37	59.59
	Xinglong Park	II	18,168.24	16,930.58	27,031.25	93,043.74	249,224.22	70.84
	Honglingjin Park	II	33,162.73	86,781.04	74,687.50	55,996.90	168,974.27	76.87
	Beixiaohe Park	I	5680.74	6042.28	6718.75	29,458.18	93,236.88	70.03
	Wanghe Park	II	6162.46	10,618.49	2031.25	62,296.59	265,490.02	50.78
	Cui Cheng Park	II	1916.55	0.00	0.00	7705.79	24,268.65	17.92

Table 2. *Cont.*

Location	Name	Type	Building and Collapsed Areas (m^2)	Water (m^2)	Slope > 7° (m^2)	Dense Area of Understory Vegetation (m^2)	Effective Refuge Area (m^2)	Percentage (%)
	Hongbo Country Park	II	5602.56	17,314.63	42,656.25	195,534.05	543,567.76	49.66
	Shungtaiba River Greenbelt	III	4080.22	0.00	1562.50	0.00	27,715.48	24.11
	Jiangfu Park	II	27,493.95	7496.87	20,781.25	82,559.15	415,388.03	92.13
	Haidian Park	I	15,598.60	19,143.41	0.00	55,628.24	240,513.02	24.61
	Yangguang Xingqiba Park	III	2831.33	1474.89	156.25	12,087.68	40,209.90	64.41
	Ninety-nine Felt Houses Fushi Road Store Green Space	III	4668.30	0.00	26,875.00	0.00	73,698.20	6.53
	Primary School Attached to CNU	III	12,631.71	0.00	0.00	0.00	13,030.54	70.23
	Bayi School	II	20,318.25	0.00	2343.75	0.00	58,633.02	75.24
	High chool Affiliated to University of Science & Technology Beijing	III	11,784.26	0.00	625.00	0.00	22,459.81	54.53
	International Sculpture Park	I	47,629.17	10,535.09	781.25	51,437.08	260,451.78	65.02
	Langfa Park	II	1751.07	0.00	2656.25	11,740.77	49,072.09	53.21
	Xinghai Park	II	3882.71	5986.02	4062.50	9831.61	28,496.74	66.71
	Subway Park	II	6916.49	0.00	12,812.50	24,247.48	81,735.73	75.38
	Wangxing Lake Park	II	948.02	13,556.52	32,343.75	52,941.23	113,494.60	43.95
	Nanyuan Park	I	4818.32	582.27	781.25	16,454.37	74,517.49	76.70

4.2. Effectiveness Analysis Results

According to Formula (2), the open space ratio of the shelter can be obtained based on the effective refuge area and the area occupied by the emergency shelter calculated in the previous section.

According to the planning and design standards for domestic and foreign emergency shelters, the per capita effective refuge area is generally 1 m^2–3 m^2. The emergency shelters studied in this paper are divided into types I, II, and III [44]. On the basis of the level of the shelter, the per capita effective refuge area is set to 2 m^2 for type I emergency shelters, 1.5 m^2 for type II emergency shelters, and 1 m^2 for type III emergency shelters [7,39]. According to these settings, the maximum capacity of the shelter can be calculated [22].

The standards for the service radius of emergency shelters are different domestically and internationally. The "Planning Outline for Earthquake and Emergency Shelters (Outdoor) in the Central Urban Area of Beijing" stipulates that the service radius of an emergency shelter is 500 m, while the service radius for a long-term (fixed) emergency shelter is 2000 m–5000 m [5]. In reference to the above standards and the literature [7], the service radius for type I emergency shelters is set to 3000 m, type II is 2000 m, and type III is 500 m. Therefore, the impedance is set to 3000 m for type I, 2000 m for type II, and 500 m for type III when the network analysis method is used to calculate the service range of the shelters (Figure 13). The ArcGIS platform not only has powerful network analysis functions but can also perform overlay analysis using other data. Using the analysis module on the ArcGIS platform to overlay the service range with street population data can determine the number of people that need shelter within the service range. This paper assumes that the population covered by the service range of the emergency shelters in the study area is the total number of people that need shelter. On the basis of Formulas (4) and (5), the per capita accessible effective refuge area and the population allocation gap of the shelter can be obtained (Table 3, Figure 14).

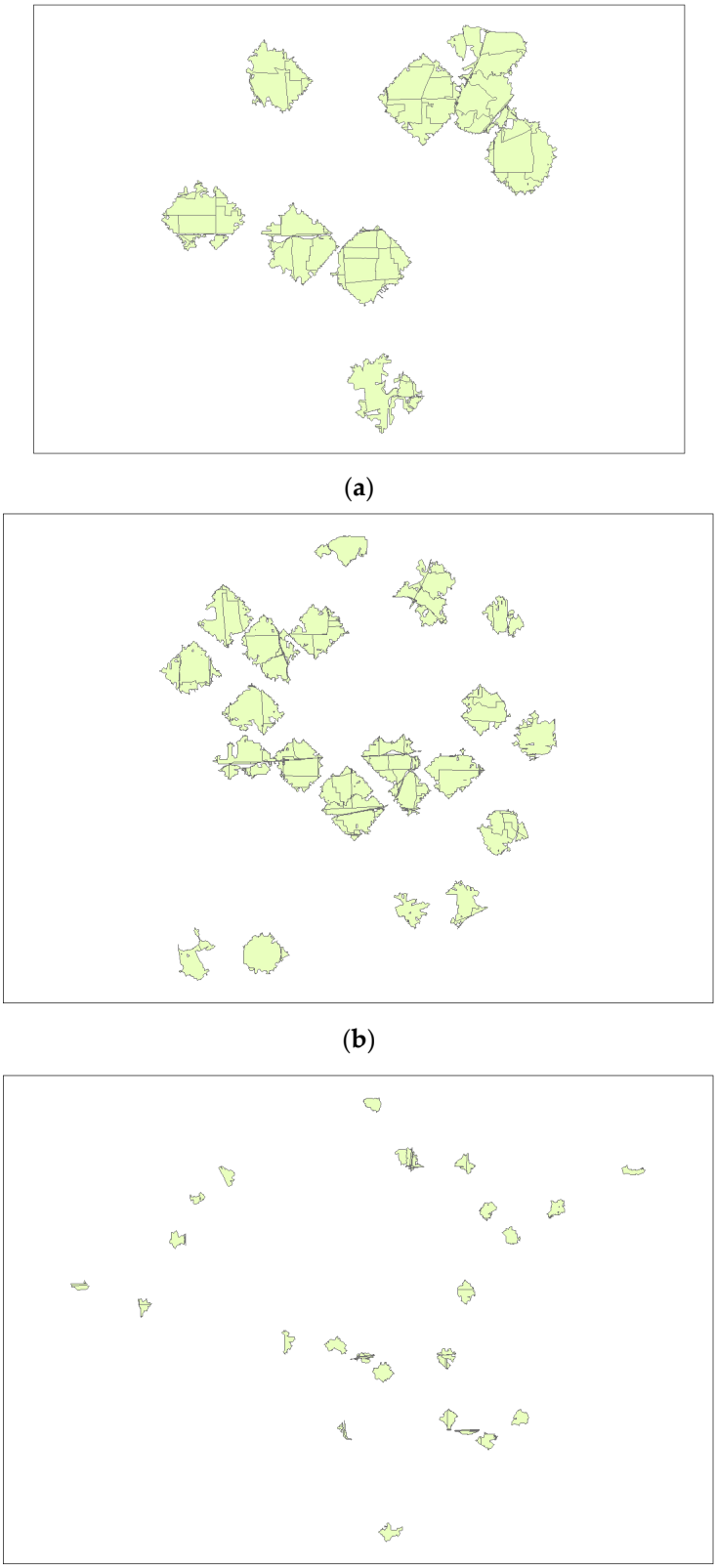

(**a**)

(**b**)

(**c**)

Figure 13. Range of services of the emergency shelters. (**a**) Range of services of type I emergency shelters. (**b**) Range of services of type II emergency shelters. (**c**) Range of services of type III emergency shelters.

Table 3. Statistics regarding the effectiveness of emergency shelters within the Fifth Ring Road of Beijing.

Location	Effective Refuge Area (m^2)	Shelter Area (m^2)	Range of Services of the Shelter (m^2)	Number of People Covered by the Service (m^2)	Open Space Ratio (%)	Capacity (Number of People)	Per Capita Accessible Effective Refuge Area (m^2)	Population Allocation Gap (Number of People)
Ring 2	939,046.74	1,740,088.14	48,514,659.97	993,778.87	53.97	808,673.85	0.94	185,105.02
Rings 2–3	297,208.52	635,949.04	32,642,904.43	698,910.67	46.73	201,369.46	0.43	497,541.21
Rings 3–4	2,016,576.86	4,243,543.16	56,554,834.18	62,767,691.39	47.52	1,086,115.90	0.03	61,681,575.49
Rings 4–5	5,281,419.62	8,068,047.20	90,503,571.38	3,423,423.87	65.46	3,468,531.20	1.54	−45,107.33

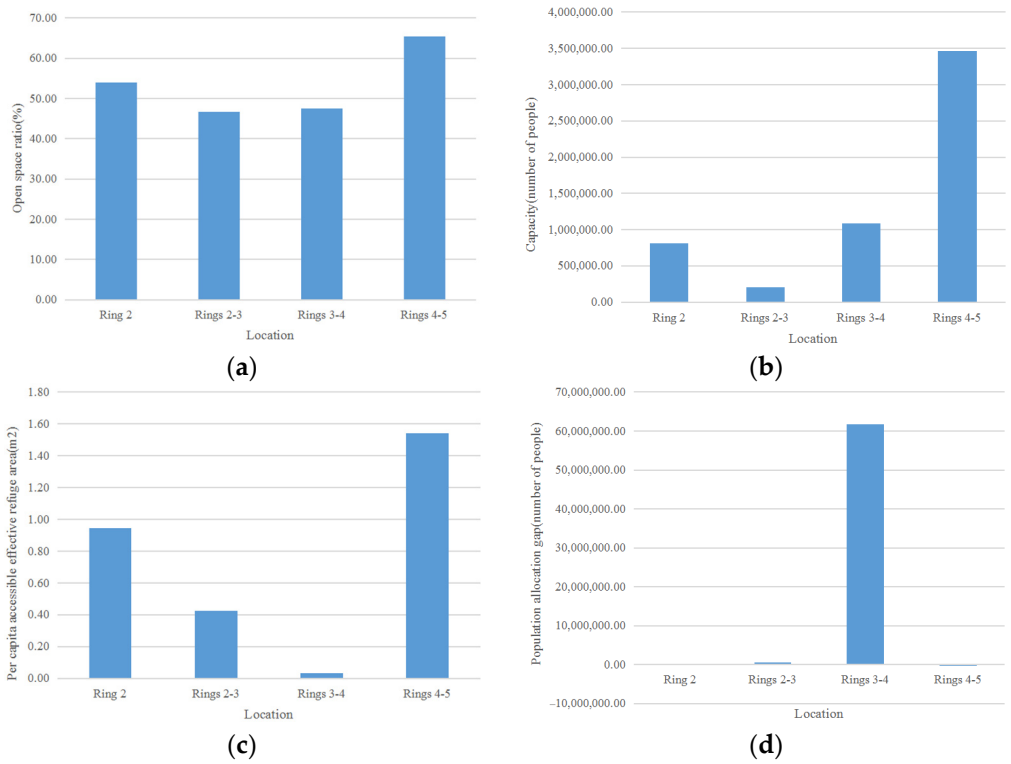

Figure 14. Analysis chart for the effectiveness of emergency shelters within the Fifth Ring Road of Beijing. (**a**) Open space ratio. (**b**) Capacity. (**c**) Per capita accessible effective refuge area. (**d**) Population allocation gap.

5. Discussion

5.1. Comparison and Verification of the Effective Refuge Area

(1) Accuracy evaluation. Four evaluation metrics—precision, recall, the F1 score, and the mean intersection over union (IoU)—were selected to verify the accuracy of the EfficientUNet+ method for building extraction [45,46]. The evaluation results are shown in Table 4.

Table 4. Accuracy verification of the EfficientUNet+ method for building extraction.

Precision (%)	Recall (%)	F1 Score (%)	mIoU (%)
93.01	89.17	91.05	90.97

Table 4 shows that the evaluation metrics of precision, recall, the F1 score, and the mean IoU reached more than 90%, indicating high accuracy in building extraction using

the EfficientUNet+ method. Therefore, the EfficientUNet+ method is effective in extracting buildings for emergency shelters.

Representative emergency shelters, including Olympic Forest Park and Chaoyang Park, were selected as examples to verify the accuracy of the water extraction. The accuracy was evaluated using the metrics of precision, recall, the F1 score, and the mean IoU, and the results are shown in Table 5.

Table 5. Accuracy evaluation of water extraction.

Emergency Shelter	Precision (%)	Recall (%)	F1 Score (%)	mIoU (%)
Olympic Forest Park	90.61	96.38	93.41	92.83
Chaoyang Park	93.75	97.45	95.56	95.18

Table 4 shows that the evaluation metrics of precision, recall, the F1 score, and the mean intersection IoU reached more than 90%, indicating high accuracy in water extraction for emergency shelters when using the object-oriented classification method developed in this study.

The proportions of trees and shrubs recorded in the related literature were used as a reference to verify the extraction results of the dense areas of understory vegetation obtained from the experiment designed in this study. Hu et al. [47] argued that the common ratio of trees to shrubs in Beijing is 7:3. Zhang et al. [48] studied the tree–shrub ratios in different types of green spaces in Beijing and found that the ratios were diverse, ranging from 1:100 to 1:10. The experimental and computational methods designed in this study found that the proportion of dense areas of understory vegetation areas in emergency shelters within the Fifth Ring Road of Beijing to the area of green space other than grass is 29.66%, which is within a reasonable range.

In conclusion, the results of extracting buildings and collapsed areas, water, and dense areas of understory vegetation using the proposed method demonstrated high accuracy and reasonability. Therefore, the effective refuge area obtained using this method is also highly precise, which demonstrates that the proposed technical system for monitoring effective refuge areas for emergency shelters is accurate, scientific, and effective.

(2) Comparison and verification. The effectiveness of the technical system for monitoring effective refuge areas proposed in this study was validated by using statistical data of effective refuge areas from the Beijing Emergency Management Bureau for comparison validation. The accuracy was evaluated using the mean absolute error (MAE) and the root mean square error (RMSE).

MAE reflects the average of the absolute error between predicted values and true values, while RMSE reflects the standard deviation of the differences between predicted values and true values. The calculated MAE and RMSE were 3.27 and 5.12, respectively, indicating that the effective shelter area calculated by the proposed method is roughly consistent with the official data. However, the remote sensing monitoring technology used in this study can accurately and efficiently obtain effective refuge areas in real time. This can provide more scientific, effective, and reasonable supporting data for locating emergency shelters and generating suitability evaluation applications. The results can also identify areas for improvement in existing disaster prevention measures and reduction plans and increase the safety of the city.

5.2. Effectiveness Analysis

(1) General analysis. In total, 59 emergency shelters are present within the Fifth Ring Road of Beijing, with a total effective shelter area of 8,534,251.76 m^2. (1) A consideration of the type of shelters shows that the area has 9 type I shelters with a total effective shelter area of 2,708,265.24 m^2; 23 type II shelters with a total effective shelter area of 4,846,286.19 m^2; and 27 type III shelters with a total effective shelter area of 979,700.33 m^2. (2) Regarding the type of emergency shelters, there are 46 park-type shelters with a total effective shelter area of 8,147,855.17 m^2; 4 green-space-type shelters with a total effective

shelter area of 243,895.85 m^2; and 9 sports-field-type shelters with a total effective shelter area of 142,500.74 m^2. Types II and III shelters are the main types of emergency shelters within the Fifth Ring Road of Beijing, meeting the short-term shelter needs of residents, whereas type I shelters are few in number. The number of park-type shelters is relatively large and they can be used for both leisure and emergency shelter purposes.

On the basis of the effective refuge area data, population data from the Seventh National Census Bulletin, and road network data from Beijing City, the following conclusions can be reached: (1) The emergency shelters within the Fifth Ring Road of Beijing can effectively accommodate 5,564,690.41 people, with the Olympic Forest Park emergency shelter having the highest capacity and the Qianmen Jianlou Green Space emergency shelter having the lowest capacity. (2) The total service area of Beijing's emergency shelters within the Fifth Ring Road is 228,215,969.95 m^2, with the Yuan Dadu City Wall Ruins Park emergency shelter having the largest service area and the Metro Park emergency shelter having the smallest. Within a certain service radius, the emergency shelters within the Fifth Ring Road can cover a population of 67,883,804.80 people, with the Xidawang Road Community Park emergency shelter serving the most people (62,037,375.70) and the Changchun Fitness Park emergency shelter serving the fewest (61.31), indicating a significant difference in the service radius and population coverage of each shelter. (3) From the perspective of population allocation gaps, only about 52.54% of the emergency shelters can meet the needs of refugees, whereas 47.46% cannot. In particular, the Xidawang Road Community Park emergency shelter area has the largest population allocation gap, which may be related to the density of the population. This finding further shows that emergency shelters within the Fifth Ring Road of Beijing exhibit regional deficiencies. Therefore, shelter distribution and spatial planning should be considered based on the population distribution to better meet the needs of local urban development.

(2) Ring scale analysis. Considering that the distribution of Beijing is centered around the Forbidden City, forming urban road networks such as Ring 2, Ring 3, Ring 4, and Ring 5 outward, and that the population distribution between the Rings is relatively dense, this paper analyzes the effectiveness of emergency shelters from the perspective of the ring area, combined with the population of streets and the effective refuge area.

In total, 18 emergency shelters are found within Ring 2, occupying an area of 1,740,088.14 m^2, with an effective refuge area of 939,046.74 m^2 and a service area of 48,514,659.97 m^2. Compared with the other ring areas, Ring 2 has a larger number of type III shelters, which can effectively accommodate 808,673.85 people. The population allocation gap is smaller, and the per capita accessible effective refuge area is relatively large, with a larger open space ratio. This finding indicates that the effectiveness of shelters within Ring 2 is relatively good overall.

Moreover, eight emergency shelters are found within Rings 2–3, occupying an area of 635,949.04 m^2, with an effective refuge area of 297,208.52 m^2 and a service area of 32,642,904.43 m^2. Compared with the other ring areas, Rings 2–3 have the smallest area of emergency shelters, effective refuge area, service range, service population, open space ratio, accommodated population, and per capita accessible effective refuge area. Although a population allocation gap exists within Rings 2–3, there are more shelters than in Ring 2, indicating that the effectiveness of shelters within Rings 2–3 is relatively poor. The possibility of increasing or developing new shelters could be considered, such as by reasonably planning and allocating open spaces such as community parks and green spaces or evacuating some of the population according to urban functional zones.

Twelve emergency shelters are found within Rings 3–4, occupying an area of 4,243,543.16 m^2, with an effective refuge area of 2,016,576.86 m^2 and a service area of 56,554,834.18 m^2. Compared with the other ring areas, Rings 3–4 have a greater number of type I shelters, which can effectively accommodate 1,086,115.90 people. Although the service range covers the most people for all the ring areas, the per capita accessible effective refuge area is the smallest, and the population allocation gap is the largest in the research area. This finding indicates that the spatial distribution of shelters within Rings 3–4 is

uneven, and the spatial and resource utilization of the shelters has not been fully utilized. Existing shelters can be replanned to meet the population's shelter needs.

Finally, 21 emergency shelters are found within Rings 4–5, occupying an area of 8,068,047.20 m^2, with an effective refuge area of 5,281,419.62 m^2 and a service area of 90,503,571.38 m^2. Compared with the other ring areas, Rings 4–5 have the largest service range but a smaller service population, indicating a relatively low population density. Based on the other indicators of effectiveness, the effective refuge area, shelter area, open space ratio, accommodated population, and per capita accessible effective refuge area are the largest, and no population allocation gap exists, indicating that the effectiveness of shelters within Rings 4–5 is relatively good. Thus, the effective refuge needs of the current population can be met while also considering possible future population changes brought about by the outflow of people from the capital's core functional area.

6. Conclusions

This paper presents a system based on the remote sensing monitoring technique for assessing the effective refuge area of emergency shelters from fine scales based on multi-source data. On the basis of the effective refuge area, this paper constructs effectiveness analysis criteria, including the open space ratio, capacity, the per capita accessible effective refuge area, and the population allocation gap. Validation was conducted in the Beijing area within the Fifth Ring Road. The main conclusions are as follows:

(1) On the basis of multi-source data, including satellite remote sensing data, aerial remote sensing, and Baidu electronic maps, this paper proposes a remote sensing monitoring method for assessing the effective refuge area of emergency shelters. Compared with the traditional estimation method, which calculates the effective refuge area to comprise 60% of the shelter area, this method can quickly and accurately monitor the dynamic changes in the effective refuge area of urban shelter sites.

(2) The extraction scale of the effective refuge area proposed in this paper is relatively fine. On the basis of the characteristics of buildings, water, the dense areas of understory vegetation, and slopes, which cannot serve as refuge spaces, a combination of deep learning, machine learning, field investigation, and GIS technology was used to intelligently extract the effective refuge area with high accuracy and efficiency. The results of extracting the effective refuge area in Beijing show that Rings 2–3 have the smallest effective refuge area and Rings 4–5 have the largest effective refuge area.

(3) Combining the effective refuge area, the actual road network, and the population distribution data, this paper constructs effective analysis criteria for emergency shelters, which includes the open space ratio, capacity, the per capita accessible refuge area, and the population allocation gap. This study provides a comprehensive, objective, and scientific method for assessing the effectiveness of emergency shelters in the Beijing area within the Fifth Ring Road. The analysis of the effectiveness results at the regional scale shows that the effectiveness of shelters is generally good within Ring 2 and is poor within Rings 2–3, exhibiting population overcrowding and inadequate refuge space. The effectiveness within Rings 3–4 is moderate with an uneven spatial distribution, while the effectiveness within Rings 4–5 is generally good with no population allocation gap.

Data acquisition was limited, which is why the population allocation gap was estimated according to the number of people covered by the service area as the requirement of refuge space. Realistic situations, such as different earthquake levels, population movements during day and night, and other factors, were not considered. In addition, there is a cumulative error in the extraction of the effective refuge area of emergency shelters from different features, which can have an impact on the population allocation gap for effective analysis. Therefore, in future research, natural environment, surrounding facilities, and different scenarios will be considered to conduct a more detailed and comprehensive evaluation of the shelters, such as load capacity analysis, population evacuation, etc.

Author Contributions: Conceptualization, D.Y., F.W. and S.W.; methodology, Z.W., D.Y., F.W. and S.W.; software, D.Y. and Z.W.; validation, Y.X., F.W. and S.W.; formal analysis, D.Y.; investigation, D.Y. and Y.W.; resources, F.W; data curation, J.W., J.J. and Y.X.; writing—original draft preparation, D.Y.; writing—review and editing, S.W.; visualization, F.W. and Z.W.; supervision, S.W. and Y.Z.; project administration, D.Y. and S.W.; funding acquisition, D.Y. and S.W. All authors have read and agreed to the published version of the manuscript.

Funding: This research was funded by the National Key R&D Program of China (No. 2021YFB3901201).

Data Availability Statement: The data presented in this study are available on request from the corresponding author.

Acknowledgments: We would like to express our gratitude to Wuhan University for providing the aerial building dataset, the researcher Zhiyu Xu for providing the Beijing green space dataset from GF-2 imagery, and the Beijing Municipal Emergency Management Bureau and Beijing Earthquake Administration for providing information on emergency shelters. We would also like to thank the anonymous reviewers and the editors for their insightful comments and helpful suggestions.

Conflicts of Interest: The authors declare no conflict of interest.

References

1. Dai, Q.; Gao, Z.; Yang, Q. Research methods for urban emergency shelters: A review. *Sci. Technol. Inf.* **2010**, *6*, 250–251.
2. Ekaputra, R.; Lee, C.; Kee, S.; Yee, J. Emergency Shelter Geospatial Location Optimization for Flood Disaster Condition: A Review. *Sustainability* **2022**, *14*, 12482. [CrossRef]
3. Wang, Y.; Xu, Z. An Emergency Shelter Location Model Based on the Sense of Security and the Reliability Level. *J. Syst. Sci. Syst.* **2023**, *32*, 100–127. [CrossRef]
4. Zhong, G.; Lu, Y.; Chen, W.; Zhai, G. Multi-objective optimization approach of shelter location with maximum equity: An empirical study in Xin Jiekou district of Nanjing, China. *Geomat. Nat. Hazards Risk* **2023**, *14*, 2165973. [CrossRef]
5. Jing, J. Beijing Municipal Planning Commission announced the 'Outline of Planning for Earthquake and Emergency Refuge Places (Outdoor) in Beijing Central City'. *Urban Plan. Newsl.* **2007**, *21*, 1.
6. Li, J.; Zhou, C.; Rong, B. Planning and Construction of Urban Earthquake Emergency Shelter Areas—Taking Beijing Earthquake Emergency Shelter Areas as an Example. *Beijing Plan. Rev.* **2008**, *4*, 16–21.
7. Wei, B.; Tan, Q.; Li, X. Assessment on spatial distribution and service efficiency of emengency shelters in Beijing. *J. Seismol. Res.* **2019**, *42*, 295–303+306.
8. Wang, X.; Guan, M.; Dong, C.; Wang, J.; Fan, Y.; Xin, F.; Lian, G. A Multi-Indicator Evaluation Method for Spatial Distribution of Urban Emergency Shelters. *Remote Sens.* **2022**, *14*, 4649. [CrossRef]
9. Tong, Y. *Research on Construction and Management of Public Park with Function of Emergency and Avoid the Danger in Beijing*; Beijing Forestry University: Beijing, China, 2010.
10. Lv, W.; Han, Y.; Zhou, W.; Shi, S. Study on the spatial correlation between the suitability evaluation of emergency shelters and the service scope. *J. Saf. Environ.* **2023**, *23*, 694–703.
11. Guo, X.; Li, H.; Li, R. Research on accessibility of emergency shelters in megacity parks—Taking Nankai district of Tianjin as an example. *Tianjin Sci. Technol.* **2021**, *48*, 57–59.
12. Zhou, A.; Shen, L.; Zhu, H.; Chen, S. Reasonability of spatial distribution for urban emergency shelter in central district of Beijing at community scale. *J. Saf. Environ.* **2021**, *21*, 1662–1669.
13. Zhang, J. Calculation of Effective Shelter Area and Prediction of Shelter Population in Urban Green Space of Urumqi. *Contemp. Hortic.* **2018**, *11*, 170–172.
14. Xiao, H. *Effectiveness Research of the Urban Primary and Secondary Emergency Shelter*; Southwest University of Science and Technology: Mianyang, China, 2017.
15. Du, H.; Lin, X.; Lu, Y.; Zhang, F.; Zhang, X.; Xu, J.; He, S. Study on the rapid extraction model of post-earthquake shelter sites based on remote sensing images: A case study of the Yangbi MS6. 4 Earthquake. *J. Seismol. Res.* **2023**, *46*, 116–127.
16. Chen, W.; Fang, Y.; Zhai, Q.; Wang, W.; Zhang, Y. Assessing Emergency Shelter Demand Using POI Data and Evacuation Simulation. *Int. J. Geo-Inf.* **2020**, *9*, 41. [CrossRef]
17. Ommi, S.; Janalipour, M. Selection of shelters after earthquake using probabilistic seismic aftershock hazard analysis and remote sensing. *Nat. Hazards* **2021**, *113*, 345–363. [CrossRef]
18. Zhao, L.; Li, H.; Sun, Y.; Huang, R.; Hu, Q.; Wang, J.; Gao, F. Planning Emergency Shelters for Urban Disaster Resilience: An Integrated Location-Allocation Modeling Approach. *Sustainability* **2017**, *9*, 2098. [CrossRef]
19. Xiong, J. *Study on Effectiveness Evaluation of Urban Disaster Prevention Park Based on F AHP—Take Nanchang People's Park as An Example*; Nanchang University: Nanchang, China, 2019.
20. Yao, Y.; Zhang, Y.; Yao, T.; Wong, K.; Yeu Tsou, J.; Zhang, Y. A GIS-Based System for Spatial-T emporal Availability Evaluation of the Open Spaces Used as Emergency Shelters: The Case of Victoria, British Columbia, Canada. *ISPRS Int. J. Geo-Inf.* **2021**, *10*, 63. [CrossRef]

21. Yu, J.; Zhang, C.; Wen, J.; Li, W.; Liu, R.; Xu, H. Integrating multi-agent evacuation simulation and multi-criteria evaluation for spatial allocation of urban emergency shelters. *Int. J. Geogr. Inf. Sci.* **2018**, *32*, 1884–1910. [CrossRef]
22. Alawi, M.; Chu, D.; Hammad, S. Resilience of Public Open Spaces to Earthquakes: A Case Study of Chongqing, China. *Sustainability* **2023**, *15*, 1092. [CrossRef]
23. Chen, P.; Zhang, J.; Zhang, L.; Sun, Y.; Liu, X. Analysis of the suitability of urban earthquake emergency refuge suitability comprehensive evaluation model and its empirical research. *Environ. Eng.* **2016**, *34*, 1132–1136.
24. Chen, J.; Xia, M.; Wang, D.; Lin, H. Double Branch Parallel Network for Segmentation of Buildings and Waters in Remote Sensing Images. *Remote Sens.* **2023**, *15*, 1536. [CrossRef]
25. Ma, Z.; Xia, M.; Weng, L.; Lin, H. Local Feature Search Network for Building and Water Segmentation of Remote Sensing Image. *Sustainability* **2023**, *15*, 3034. [CrossRef]
26. Liu, B.; Du, S.; Bai, L.; Ouyang, S.; Wang, H.; Zhang, X. Water extraction from optical high-resolution remote sensing imagery: A multi-scale feature extraction network with contrastive learning. *GISci. Remote Sens.* **2023**, *60*, 2166396. [CrossRef]
27. Xu, Z.; Zhou, Y.; Wang, S.; Wang, L.; Li, F.; Wang, S.; Wang, Z. A Novel Intelligent Classification Method for Urban Green Space Based on High-Resolution Remote Sensing Images. *Remote Sens.* **2020**, *12*, 3845. [CrossRef]
28. Xu, Z.; Zhou, Y.; Wang, S.; Wang, L.; Wang, Z. U-Net for urban green space classification in Gaofen-2 remote sensing images. *J. Image Graph.* **2021**, *26*, 0700–0713.
29. You, D.; Wang, S.; Wang, F.; Zhou, Y.; Wang, Z.; Wang, J.; Xiong, Y. EfficientUNet+: A Building Extraction Method for Emergency Shelters Based on Deep Learning. *Remote Sens.* **2022**, *14*, 2207. [CrossRef]
30. Tadepalli, Y.; Kollati, M.; Kuraparthi, S.; Kora, P. EfficientNet-B0 Based Monocular Dense-Depth Map Estimation. *Trait. Signal* **2021**, *38*, 1485–1493. [CrossRef]
31. Alhichri, H.; Alswayed, A.S.; Bazi, Y.; Ammour, N.; Alajlan, N.A. Classification of Remote Sensing Images using EfficientNet-B3 CNN Model with Attention. *IEEE Access* **2021**, *9*, 14078–14094. [CrossRef]
32. Zhang, D.Q.; Li, D.; Zhou, L.; Wu, J. Fine Classification of UAV Urban Nighttime Light Images Based on Object-Oriented Approach. *Sensors* **2023**, *23*, 2180. [CrossRef]
33. Wei, S.; Luo, M.; Zhu, L.; Yang, Z. Using object-oriented coupled deep learning approach for typical object inspection of transmission channel. *Int. J. Appl. Earth Obs. Geoinf.* **2023**, *116*, 103137. [CrossRef]
34. Fu, N.; Zou, Z. Research on the application of middle and lower level garden plants in real estate landscape. *Chin. Hortic. Abstr.* **2013**, *29*, 54–56.
35. Ren, J.; Li, W.; Wang, J.; Cui, H.; Shan, S. Study on spatial layout of earthquake emergency shelter in Dawukou district of Ningxia. *J. Disaster Prev. Reduct.* **2021**, *37*, 61–67.
36. Wigati, S.; Sopha, B.; Asih, A.; Sutanta, H. Geographic Information System Based Suitable Temporary Shelter Location for Mount Merapi Eruption. *Sustainability* **2023**, *15*, 2073. [CrossRef]
37. Hosseini, K.A.; Tarebari, S.A.; Mirhakimi, S.A. A new index-based model for site selection of emergency shelters after an earthquake for Iran. *Int. J. Disaster Risk Reduct.* **2022**, *77*, 103110. [CrossRef]
38. Liu, S.; Lu, Y.; Gu, X.; Pei, Y.; Liu, T. Reasonability of spatial distribution for urban emergency shelter. *Urban Dev. Stud.* **2012**, *19*, 113–117+120.
39. Chu, J. *Research on the Methods for Planning of Emergency Shelter and Its Application*; Tianjin University: Tianjin, China, 2014.
40. Li, Y.; Chen, T.; Zang, X. GIS-supported research on urban earthquake emergency response capacity. *World Earthq. Eng.* **2018**, *34*, 1–9.
41. Şenik, B.; Uzun, O. An assessment on size and site selection of emergency assembly points and temporary shelter areas in Düzce. *Nat. Hazards* **2021**, *105*, 1587–1602. [CrossRef]
42. Ji, J.; Gao, X. Evaluation method and empirical study on service quality of seismic emergency shelters. *Geogr. Res.* **2014**, *33*, 2105–2114.
43. Liu, C.; Liu, S.; Zhang, J.; Wang, L.; Guo, X.; Li, G.; Wang, W. An optimal design method of emergency evacuation space in the high-density community after earthquake based on evacuation simulation. *Nat. Hazards* **2023**, *116*, 2889–2915. [CrossRef]
44. Zhang, X.; Yu, J.; Chen, Y.; Wen, J.; Chen, J.; Yin, Z. Supply–Demand Analysis of Urban Emergency Shelters Based on Spatiotemporal Population Estimation. *Int. J. Disaster Risk Sci.* **2020**, *11*, 519–537. [CrossRef]
45. Ji, S.; Wei, S.; Lu, M. Fully convolutional networks for multisource building extraction from an open aerial and satellite imagery data set. *IEEE Trans. Geosci. Remote Sens.* **2018**, *57*, 574–586. [CrossRef]
46. Wei, S.; Ji, S.; Lu, M. Toward automatic building footprint delineation from aerial images using cnn and regularization. *IEEE Trans. Geosci. Remote Sens.* **2019**, *58*, 2178–2189. [CrossRef]
47. Hu, J.; Wu, Y.; Zhang, Y. Planting design of Beijing Olympic Forest Park. *Chin. Landsc. Archit.* **2006**, *6*, 25–31.
48. Zhang, X.; Li, Z.; Wang, L.; Zhao, C.; Liu, Y. Analysis of the ratio of arbor to shrub of several types of green space in Beijing. *J. Beijing For. Univ.* **2010**, *32*, 183–188.